

# **Lawrence Berkeley National Laboratory**

## Lawrence Berkeley National Laboratory

**Title**

Entangled Solid-State Circuits

**Permalink**

<https://escholarship.org/uc/item/47w7s9m4>

**Authors**

Siddiqi, Irfan  
Clarke, John

**Publication Date**

2006-08-09

## Entangled Solid-State Circuits

I. Siddiqi and John Clarke

A fundamental tenet of quantum mechanics is the idea that two spatially separated objects exhibit correlations in observable physical properties that cannot be explained by any classical theory. Troubling even Einstein, this “spooky action at a distance” (1)—known as entanglement—is fundamental to quantum information science and directly related to the enhanced computing power of a processor based on quantum bits (qubits). What is remarkable is that solid-state electrical circuits containing as many as  $10^{11}$  atoms can be engineered to exhibit quantum behavior and are well described by the quantum formalism originally developed for individual atoms and photons. One can construct such qubits from thin films using techniques developed in the semiconductor industry for conventional microelectronic circuits, thus making them attractive candidates for eventually realizing a quantum computer with many qubits.

With these solid-state “atoms on a chip” one can prepare arbitrary superpositions of single-qubit states and manipulate them with microwave radiation to observe the Rabi oscillations, Ramsey fringes and echoes long-familiar in atomic physics and nuclear magnetic resonance (NMR) (2-5). Coupling two or more qubits together results in entangled states with energy spectra that exhibit the avoided crossings (anticrossings) (6) predicted by quantum mechanics. Verifying that two qubits are unambiguously entangled is, however, a delicate task, and requires sophisticated benchmarks such as state tomography (7). This method involves a series of measurements to reconstruct the density matrix that specifies the components of an arbitrary quantum state. In a significant advance, on page yyy Steffen *et al.* (8) report the first tomographic measurements of an entangled state produced by two coupled solid-state qubits.

Steffen *et al.* use two superconducting phase qubits, A and B, coupled by a capacitance  $C_x$ , as shown in Fig. 1A. Each qubit consists of a Josephson tunnel junction—shunted with a capacitance C—in a superconducting loop of inductance L. The dynamics of the system are described by the motion of a fictitious particle representing the quantum variable  $\delta$ , the difference between the phases of the superconducting order parameters on each side of the junction. This particle is confined to an asymmetric double-well potential  $U(\delta)$  formed by applying an external magnetic flux (Fig. 1B). The two lowest energy levels in the shallow potential well on the left are the quantum states  $|0\rangle$  and  $|1\rangle$  of the phase qubit, separated by energy  $E_{01}$ . Fast pulses of microwaves at frequency  $E_{01}/\hbar$  prepare any chosen superposition of  $|0\rangle$  and  $|1\rangle$ ; transitions from  $|1\rangle$  to  $|2\rangle$  can be ignored because their energy difference is off-resonance. Once state preparation is complete, a fast flux pulse tilts the potential as shown in Fig. 1C. If the qubit is in the state  $|1\rangle$ , the phase particle tunnels to the adjacent deep potential well, causing a sudden change in  $\delta$  and inducing a magnetic flux that is stored in the loop. If the qubit is initially in the state  $|0\rangle$ , however, no tunneling occurs. The difference between these two

flux states is readily detected with an on-chip SQUID (Superconducting QUantum Interference Device) inductively coupled to the qubit.

In the case of two coupled phase qubits, there are four basis states,  $|00\rangle$ ,  $|01\rangle$ ,  $|10\rangle$ , and  $|11\rangle$ ; 0 and 1 indicate the state of each individual qubit. In their experiment, Steffen *et al.* prepare the entangled state  $(|01\rangle - i|10\rangle)/\sqrt{2}$ , one of the states that is important in quantum logic. The density operator for this state, which contains the amplitudes projected on the basis vectors, is  $\hat{\rho} = (|01\rangle - i|10\rangle)(\langle 01| + i\langle 10|)/2$ . The corresponding density matrix is

$$\rho = \begin{matrix} & \begin{matrix} |00\rangle & |01\rangle & |10\rangle & |11\rangle \end{matrix} \\ \begin{matrix} \langle 00| & \langle 01| & \langle 10| & \langle 11| \end{matrix} & \begin{pmatrix} 0 & 0 & 0 & 0 \\ 0 & 1/2 & -i/2 & 0 \\ 0 & i/2 & 1/2 & 0 \\ 0 & 0 & 0 & 0 \end{pmatrix} \end{matrix} \quad (1)$$

Entanglement is indicated by the non-zero, off-diagonal elements of the density matrix,  $i/2$  and  $-i/2$ ; these particular off-diagonal matrix elements must be non-zero to represent an entangled state. If one instead had a product state of the form  $(|10\rangle + |00\rangle)/\sqrt{2} = (|1\rangle + |0\rangle)|0\rangle/\sqrt{2}$ , there would be no quantum correlations between measurements of the states of the first and second qubits. Simply measuring qubit A, for example, cannot distinguish between the entangled and product states described above, and each measurement would yield a 50% probability to be in  $|0\rangle$  or  $|1\rangle$ . A more sophisticated sequence, namely state tomography, is needed to determine all the elements of the density matrix.

Arguably, George Stokes (9) introduced such a procedure in 1852 in the context of linear optics. Using a set of four measurements involving polarizers of various orientations, he reconstructed the polarization state of an unknown electromagnetic wave. In the case of coupled phase qubits, a tomographic measurement involves applying different NMR style microwave pulse sequences prior to readout to obtain different linear combinations of the elements of the density matrix (10). From this information, Steffen *et al.* reconstruct the density matrix using a least-squares fitting algorithm. Their results convincingly show the signatures of their entangled state, namely the diagonal and non-zero off-diagonal matrix elements shown in Eq.(1). After correction for known measurement errors, the observed magnitudes are 87% of the theoretical values. The remaining discrepancy is consistent with predictions based on the measured decoherence time.

These tomographic measurements are a positive step forward for solid-state quantum computing, representing a proof-of-principle demonstration of the basic functions needed for a quantum computer. At the same time, we are reminded of the complexities of the solid-state which has many possible channels of decoherence. These mechanisms are not well understood and are currently the subject of intense research. Fidelity—control and measurement precision—may be lost through the interaction of the qubit with many uncontrolled degrees of freedom, for example the readout circuit, low-frequency noise in charge, flux, and junction critical current, lossy circuit materials, and cross-talk between qubits. Steffen *et al.* suggest that in their phase qubit, the observed loss of fidelity is dominated by poor dielectric materials. Decoherence in other kinds of superconducting qubits is reduced by operating them at symmetry points at which they are insensitive to environmental noise (3), thereby implementing a level of hardware fault tolerance. Moreover, quantum error correction codes have been developed for software fault tolerance. Given the tremendous progress made with superconducting qubits in the past few years, we expect the demonstration of even more sophisticated quantum algorithms in the not too distant future.

1. A. Einstein, B. Podolsky, and N. Rosen, *Phys. Rev.* **47**, 777–780 (1935).
2. Y. Nakamura, Yu. Pashkin, and J.S. Tsai, *Nature* **398**, 786 (1999).
3. D. Vion *et al.*, *Science* **296**, 886 (2002).
4. I. Chiorescu *et al.*, *Science* **299**, 1869 (2003).
5. J.R. Petta *et al.*, *Science* **309**, 2180 (2005).
6. J. Von Neumann and E. Wigner, *Z. Phys.* **30**, 467 (1929).
7. U. Leonhardt, *Phys. Rev. Lett.* **74**, 4101–4105 (1995).
8. M. Steffen *et al.* *Science* **XXX**, yyy (2006).
9. G.C. Stokes, *Trans. Cambridge Philos. Soc.* **9**, 399 (1852).
10. I.L. Chuang *et al.*, *Proc. R. Soc. Lond A* **454**, 447 (1998).

I. Siddiqi is in the Department of Physics, 366 LeConte Hall, University of California, Berkeley CA 94720-7300, USA. E-mail: [irfan\\_siddiqi@berkeley.edu](mailto:irfan_siddiqi@berkeley.edu). John Clarke is in the Department of Physics, 366 LeConte Hall, University of California, Berkeley CA 94720-7300, and the Materials Sciences Division, Lawrence Berkeley National Laboratory, One Cyclotron Road, Berkeley CA 94720, USA. E-mail: [jclarke@berkeley.edu](mailto:jclarke@berkeley.edu).

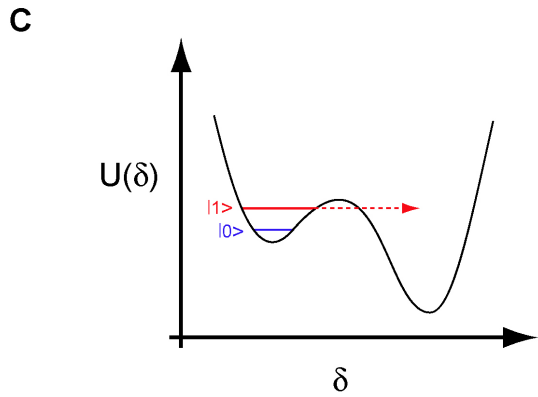
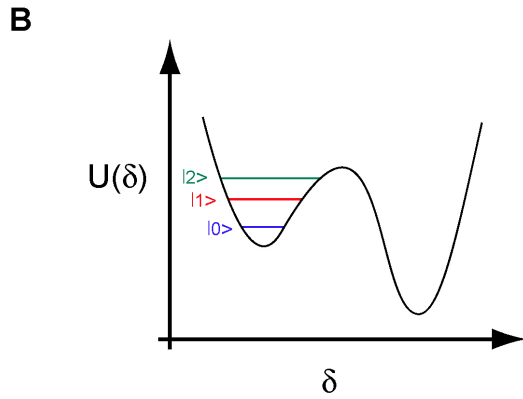
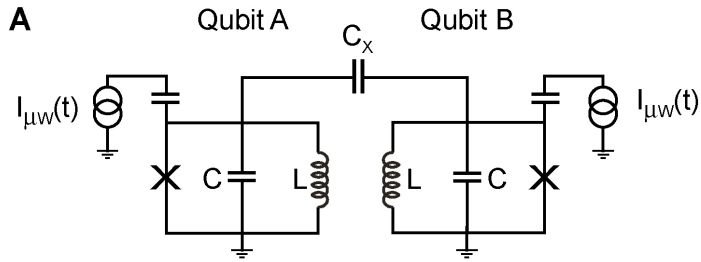


Fig. 1 Coupled superconducting phase qubits. **(A)** Simplified schematic of two phase qubits coupled via a capacitance  $C_x$ . Each qubit consists of a Josephson junction (x) shunted by a capacitance C and an inductance L. **(B)** Potential energy wells of a fictitious particle versus phase difference  $\delta$ . The barrier height and level spacing are adjusted by an external magnetic flux. Microwaves induce transitions between the states  $|0\rangle$  and  $|1\rangle$  to create any chosen superposition. **(C)** Potential energy wells with barrier height lowered by applying a fast flux pulse for qubit state measurement. If the particle is in the state in  $|1\rangle$ , it tunnels out of the left-hand well, creating a flux in the loop that is detected by a SQUID; if instead the particle is in the state  $|0\rangle$ , it does not tunnel.